Ice formation modelling around the coils of an ice storage tank

2012 J. Phys.: Conf. Ser. 395 012133

(http://iopscience.iop.org/1742-6596/395/1/012133)

Ice formation modelling around the coils of an ice storage tank

J Biosca-Taronger, J Payá, A López-Navarro and J M Corberán

Institute for Energy Engineering, Universidad Politécnica de Valencia, Camino de Vera s/n, Edificio 8E semisótano, 46022 Valencia (Spain)

e-mail: jabiota@upvnet.upv.es

Abstract. This paper aims to develop a dynamic model of the charging process of a commercial ice-storage tank. Firstly, three different 1st order and 2nd order numerical schemes have been compared to solve the transport equation of the heat transfer fluid. Euler's method has finally been chosen as the mass flow rate can vary throughout the charging and it avoids the oscillations which are introduced by Lax-Wendroff's and MacCormack's method. Secondly, the heat transfer outside the coils is analyzed. The numerical complications involved in the creation of the first ice layer around the tubes are discussed and an electrical resistance model is introduced to avoid this problem. The model results have provided a very good agreement with experimental measurements of charging tests which have been performed on a CALMAC ICEBANK tank with a capacity of 172 kWh. The model helps to predict the final part of the latent heat transfer process, where the thermal power is decreased due to the contact between the ice layers around adjacent tubes of the tank.

Nomenclature

A	cross-sectional area of the tube (m^2)	R_{ice_int}	thermal resistance of the inner half of the ice layer (K/W)
C_p	heat capacity of HTF (J/kg K)		
h	convection heat transfer coefficient (W/m^2 K)	R_{tube}	thermal resistance of the tube (K/W)
		t	time (s)
Δh_s	latent heat (J/kg)	T	temperature of HTF (K)
k_{ice}	thermal conductivity of ice (W/m K)	T_{ice}	temperature of ice (K)
$\dot{m}_{ice}$	variation of ice mass (kg/s)	T_{phase_change}	temperature of phase change interface (K)
P	inner perimeter of the tube (m)		
$\dot{Q}_{cond\_ice}$	heat conduction in the ice (W)	T_{tube}	temperature of the tube (K)
$\dot{Q}_{cond\_tube}$	heat conduction in the tube (W)	u	velocity of HTF (m/s)
$\dot{Q}_{conv\_water}$	heat convection in the water (W)	UA/L_{p_c-ice}	heat transfer coefficient between phase change interface and ice (W/m K)
$\dot{Q}_{sens\_ice}$	sensible heat in the ice (W)		
r_{ice}	radius of ice surface (m)	x	position along the tube (m)
r_{ice_m}	radius of centre of ice layer (m)		
R_{ice_ext}	thermal resistance of the external half of the ice layer (K/W)	*Greek letters*	
		ρ	HTF density (kg/m^3)

1. Introduction

Due to the increasing demand of refrigeration, a key point in the next years is to develop more efficient cold generation and storage technologies. In comparison with Sensible Heat Storage (SHS), Latent heat storage (LHS) presents the advantage of having a high volumetric capacity, and that the energy storage takes place within a fairly uniform temperature range [1-3].

Many Phase Change Materials (PCMs) are being tested [4], although in the temperature range which is useful for air-conditioning (-5 ºC to 10 ºC), there are not many options, mainly ice storage, ice slurries or paraffins with a low melting temperature. Ice storage is a low cost and a rather simple technological solution but presents the drawback in the chiller performance at the low evaporation temperatures which are required due to the subcooling of water. Ice-storage systems can be divided into external and internal-melt-ice-on-coil systems. The latter systems have been treated less in literature, especially in the case of systems with a significant capacity (above 100 kWh) and complex coil geometries.

This paper presents the development of a model for the charging of an ice-storage tank as well as the model validation with measurements from the test rig.

2. Description of the experimental ice-storage installation

A special test rig has been built at the Institute for Energy Engineering of the UPV to characterize different energy storage systems within a temperature range -10 ºC to 100 ºC [5]. The installation (shown in figure1) enables the characterization of LHS systems with different supply temperatures and mass flow rates of the heat transfer fluid (HTF). Mass flow rates between 1000 kg/h and 4000 kg/h of the HTF (26% water/glycol mixture) are achieved by means of a variable-speed pump CRE5-5 from GRUNDFOS which has a nominal power consumption of 750 W.

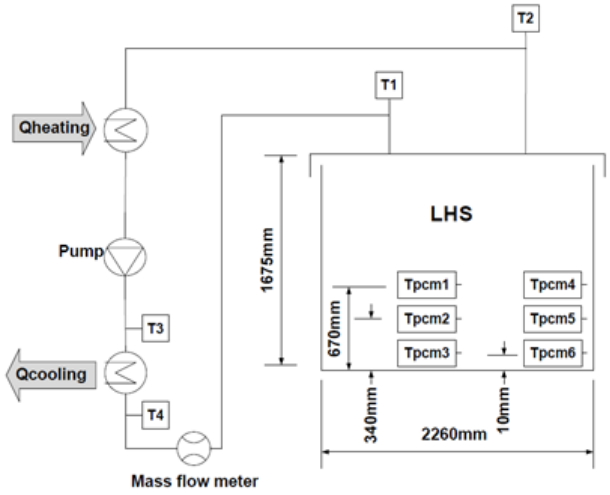

Figure 1. Layout of the experimental installation.

In order to carry out the charge and discharge tests of the ice tank, an external heat sink and source are required. The required cooling power (charge tests) is achieved with an 8 kW water-to-water chiller working with R22. The building condensation ring (water at 24.5 ºC) provides the necessary heating power for the ice-melting (discharge tests).

The LHS system is a CALMAC ICEBANK tank model 1098C [6]. The tank consists of polyethylene pipes distributed in a spiral-shape in horizontal planes. The upper and lower spirals for each plane are placed in counter-current in order to achieve more uniform temperatures within the PCM which is tap water. In total, the tank has 34 tubes immersed in the PCM. In the present work, the tank has been tested at a partial load of around 172 kWh by blocking the top 16 coils using plumbing accessories for polyethylene pipes. Thus, the HTF only circulates through the bottom 18 coils, which are the ones which are surrounded by water.

The supply and return temperatures of the HTF (T1 and T2 in figure 1) are of particular interest as they enable the calculation of the charge and discharge power. Thus, they have been measured with RTD thermal resistances PT100 1/10 DINB with an accuracy of ±0.03 K according to manufacturer data. Many other variables are also measured, for instance temperatures and pressures in the external loops, but these are out of bounds in this work.

The temperature measurements are fully monitored by means of a datalogger Agilent 34970A and three 22 channels multiplexer HP 34901A. The mass flow rate of the HTF is measured by means of a SIEMENS CORIOLIS flow meter with an uncertainty of ±7.3 kg/h.

3. Solution of the transport equation

The system which has been modelled is composed of the heat transfer fluid flowing through the tube, the tube itself and the PCM (water-ice) surrounding the tube. The aim of the model is to solve the temperature of each one of these components and the heat transfer between them at different time intervals. A one-dimensional model has been applied in order to calculate the latter temperatures along the length of the coil (x).

Firstly, the problem consists in obtaining the temperature distribution of the HTF along the tube. In order to solve the transport equation, three finite difference methods were used; the Euler's Method (a first order explicit method) and two second order explicit methods (Lax-Wendroff Method and MacCormack Method) [7]. MacCormack's Method is a variation of the two-step Lax-Wendroff scheme.

In the following paragraphs, a comparison is shown for the three methods by applying the same initial and boundary conditions. Initially both the tube and the entering fluid have a temperature of 10 ºC, and then at time t=0 s the HTF enters the coil at 2 ºC, hereby introducing a step in the temperatures of the HTF. The transport of this step through the tube length is analyzed in the following subsections.

Two cases were considered: the adiabatic case, without heat exchange between the fluid inside the tube and the tube, and the non adiabatic case, taking into account the heat exchange by convection between the fluid and the tube, which remains at a constant temperature.

3.1. Adiabatic case

In the adiabatic case, the temperature variation of the fluid along the tube is only due to the displacement of the fluid. The equation which has to be solved is hereby:

$$\frac{\partial T}{\partial t} + u\frac{\partial T}{\partial x} = 0 \tag{1}$$

Where T is the fluid temperature, t is the time, x the position along the tube and u the velocity of the fluid in the tube. In the time and spatial discretization of the differential equation (1), the coefficient CFL= $u \cdot \Delta t/\Delta x$ appears. The stability and the accuracy of the methods depend on the value of the CFL. Euler's Method, Lax-Wendroff's Method and McCormack's Method need for the stability that CFL≤1. For these reasons, in any simulation the time step and x-spacing have to be chosen carefully depending on the fluid velocity u. Euler's Method is a first order explicit method based on the following scheme:

$$T_i^{n+1} = (1 - CFL)T_i^n + CFL \cdot T_{i-1}^n \tag{2}$$

The Lax-Wendroff Method uses a scheme in two steps. Step 1 is the Lax method applied at the midpoint *i+1/2* for a half time step, and the step 2 is the leap frog method for the remaining half time step:

Step 1:
$$T_{i+1/2}^{n+1/2} = (T_{i+1}^n + T_i^n)/2 - \frac{CFL}{2}(T_{i+1}^n - T_i^n) \cdot T_{i+1}^n \tag{3}$$

Step 2:
$$T_i^{n+1} = T_i^n - CFL\left(T_{i+1/2}^{n+1/2} - T_{i-1/2}^{n+1/2}\right) \tag{4}$$

The MacCormack Method is a variation of the two-step Lax-Wendroff scheme, removing the unknown grid points *i+1/2* and *i-1/2*. Then step 1 provides a first predicted value of *T* (predictor step), and step 2 provides the final value of *T* (corrector step):

Predictor step: $$\overline{T_i^{n+1}} = (1 + CFL)T_i^n - CFL \cdot T_{i+1}^n \quad (5)$$

Corrector step: $$T_i^{n+1} = \frac{T_i^n + \overline{T_i^{n+1}}}{2} - \frac{CFL}{2}\left(\overline{T_i^{n+1}} - \overline{T_{i-1}^{n+1}}\right) \quad (6)$$

In figure 2, the progression of the temperature step is shown for the three methods. As shown in figure 2.a, for CFL=1, the results are identical for the three methods. Figures 2.b and 2.c show that for CFL<1 the Lax-Wendroff scheme and the McCormack scheme provide identical results, but different form the Euler scheme. In fact, McCormack's method is a variation of the Lax–Wendroff scheme, but is much simpler in application. Figures 2.b and 2.c show that the Euler scheme introduces a diffusion of the step and a drop of the slope, in other words a dissipation error which is typical of first order methods. The Lax-Wendroff and McCormack schemes have a steeper slope, but they introduce an oscillation to reach the steep slope of the step. This dispersion error is typical of second order methods. The oscillation becomes greater as the step moves forward along the nodes of the tube, and this can be a problem in systems with long tubes. The oscillation also becomes greater as the CFL is lowered.

3.2. Non adiabatic case

In this case, the heat transfer between the wall and the HTF is introduced by means of a constant forced convection coefficient. The transport equation with non adiabatic conditions becomes:

$$\frac{\partial T}{\partial t} = -u\frac{\partial T}{\partial x} + \frac{Ph}{\rho A C_p}(T_{tube} - T) \quad (7)$$

Where P is the inner perimeter of the tube, h is the convection coefficient, A is the cross-sectional area of the tube, ρ is the HTF density, C_p is the heat capacity and T_{tube} is the temperature of the tube. In equation (7), both T_{tube} and T are dependent on the x-coordinate.

As inferred from figure 2.d, 2.e and 2.f, the temperatures around the step are similar than for the adiabatic case, but with the exception that the fluid is progressively heated as it circulates thorough the tube, which has a higher temperature of 10ºC.

To sum up, second order methods reproduce better the slope of the step but introduce oscillations, which are greater as the fluid flows through tube and for low CFL values. This can be a problem for the modelling of ice-storage tanks as the CALMAC ICEBANK model 1098C which has rather long tubes (around 70 m) and where the mass flow rate, and consequently the CFL vary during the charge process. Nevertheless, Euler's Method introduces a diffusion of the step. Taking into account that the diffusion due to conduction inside the fluid in the axial direction and axial diffusion due to turbulence have been neglected, the diffusion introduced by the Euler's method is not problematic, since real temperature profiles are closer to Euler's solution than the theoretical step-shape. Thus, Euler's Method has been chosen to obtain the fluid temperature distribution along the tube of the tank. The outlet temperature is calculated for one single tube, although in practice the fluid in the outlet comes from a common collector from all of the coils.

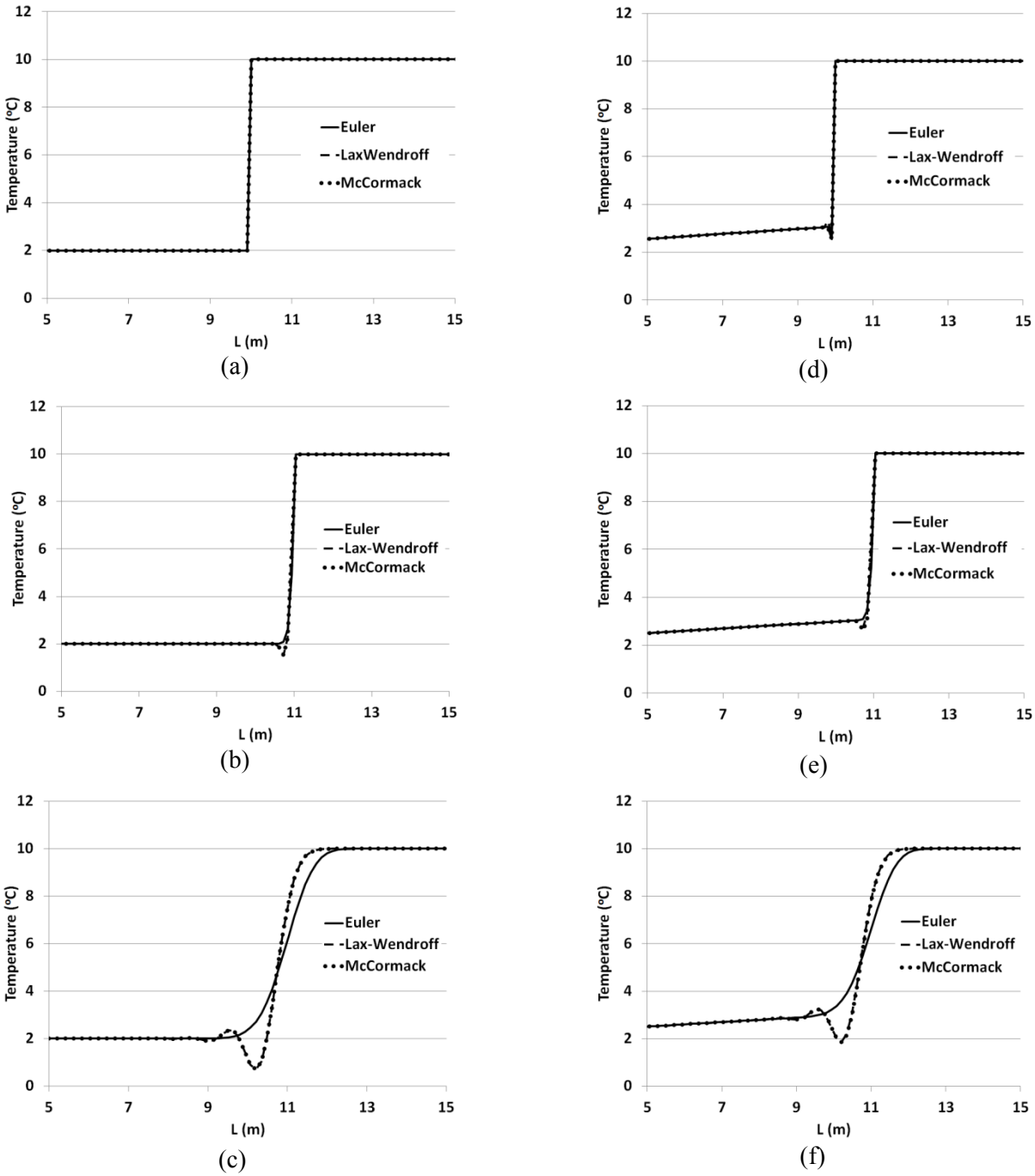

Figure 2. Fluid temperature profiles along the tube for the adiabatic case: a) CFL=1, b) CFL=0.99, c) CFL=0.8, and for the non adiabatic case: d) CFL=1, e) CFL=0.99, f) CFL=0.8.

4. Ice layer growth and heat transfer modelling

Once the transport equation has been solved for the HTF, the next step is to analyze the heat transfer within the tube (conduction), the surrounding ice layer (conduction) and the water (convection). The figure 3 shows a scheme of the ice formation process for a Δx of tube:

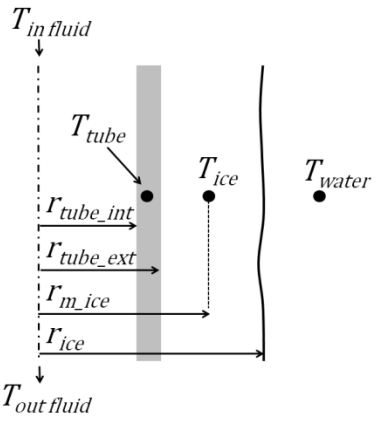

Figure 3. Scheme of the ice formation process.

The model calculates for each time step the heat transfer rates between each point, the consequent temperature, and the ice layer thickness. Heat conduction in the axial direction has been neglected for the HTF and also for the tube and the ice layer, due to the greater temperature gradient and exchange surface in radial direction than in the axial one. In further studies this effect could be studied in more detail. Thus the current model focuses in the heat transfer in the radial direction, between the fluid, the wall, the ice layer and the surrounding water. Each of these elements is represented by a single temperature node.

The interface between the ice and the water is assumed to be at 0º C. In this moving solid/liquid boundary layer, the energy balance is represented by means of equation (8):

$$\dot{Q}_{cond\_ice} = \dot{m}_{ice}\,\Delta h_s + \dot{Q}_{conv\_water} + \dot{Q}_{sens\_ice} \tag{8}$$

Where $\dot{Q}_{sens\_ice}$ is the sensible heat due to the temperature difference between the new ice layer formed at 0ºC and the mean temperature considered for the ice.

Once the first ice layer is formed, this interface is placed at the tube surface. The energy balance equation is then:

$$\dot{Q}_{cond\_tube} = \dot{m}_{ice}\,\Delta h_s + \dot{Q}_{conv\_water} \tag{9}$$

Before the first ice-layer appears, numerical problems appear for the ice temperature calculation. In fact, the heat transfer by conduction between the solid/liquid interface and the ice is calculated by means of equation (10) which depends on the ice layer thickness:

$$UA/L_{p\_c-ice}{}_i^{\,n} = \left[\frac{\ln\left(r_{ice}{}_i^{\,n}/r_{ice\_m}{}_i^{\,n}\right)}{2\pi k_{ice}}\right]^{-1} \tag{10}$$

As the ice thickness tends to 0, the previous logarithm tends to 0 and the coefficient UA/L_{p_c-ice} tends to infinite. Thus, for the instants when the ice layer thickness is less than 0.5 mm, the ice temperature is calculated by means of an electric equivalent, as represented in figure 4.

In the electric equivalent, from the temperatures of the tube and the phase-change interface, and knowing the thermal resistances between these points, the temperature of the ice node is obtained, considering the ice node placed at the centre of the ice layer. The equation which has been employed to calculate the ice temperature is shown in the equation (11). It has been assumed that the heat leaving the phase-change interface is equal to the heat transferred by the tube, as would happen in steady state. Although the charge process is completely transient, when the ice thickness is very small the heat rejected by the ice due to its temperature variation is negligible compared with the heat leaving the phase-change interface to the tube.

$$T_{ice} = T_{tube} + \left(T_{phase\_change} - T_{tube}\right)\frac{\left(R_{tube}+R_{ice\_int}\right)}{\left(R_{tube}+R_{ice\_int}\right)+R_{ice\_ext}} \tag{11}$$

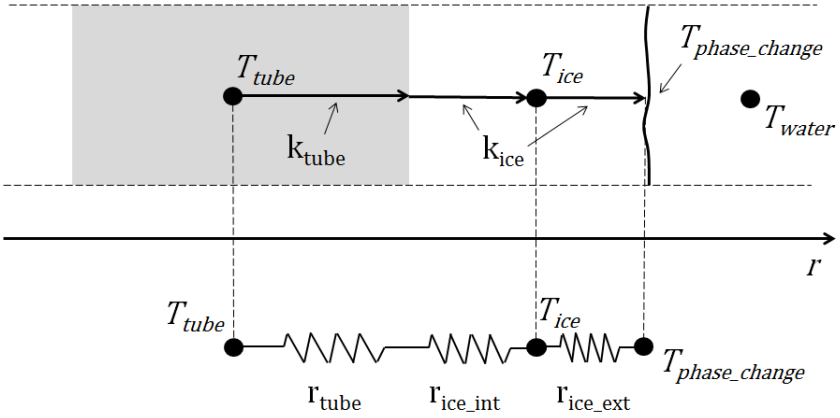

Figure 4. Scheme of the electric equivalent.

The ice-tank has a central region with a vertical supply and return collector, but with no spiral coils. Thus, this region has hardly any contact between the water and the coils. The model considers the existence of this volume of water and its mass transfer with the water nodes surrounding the coils due to the free convection of the water. The estimation of the free convection coefficient around the tube is based on the modification of the Grashof number proposed by Gebhart [8] which takes into account the density inversion of the water around 4 ºC.

The model also considers a restriction for the ice-layer growth. In fact, at the end of the charge process due to the contact between the ice layer of two adjacent tubes, the thermal power decreases.

The nucleation temperature depends on several factors like salinity or the existence of nucleation agents or surfaces, and it is also a very random process even for same inlet conditions of the HTF [9]. Thus, in the model the nucleation temperature is an input from the experimental tests.

5. Validation

In this section, the developed model has been validated with tests from the experimental test rig. Several tests have been carried out to study the performance of the ice-storage tank with different inlet mass flow rates and temperatures for the HTF. Figure 5 shows a comparison of the outlet temperature of the HTF for a test with a mass flow rate of 3500 kg/h. In this test, nucleation was experimentally observed at a mean temperature of -0.5º C.

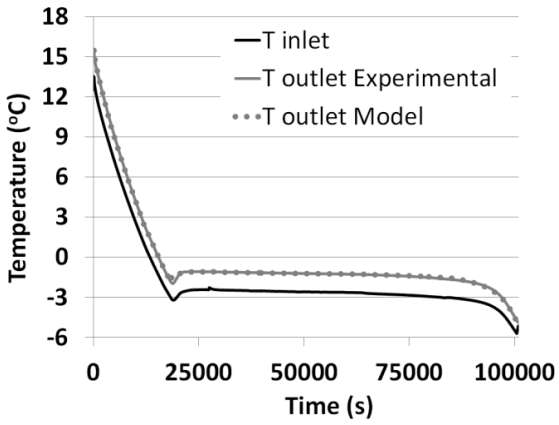

Figure 5. Temperature comparison.

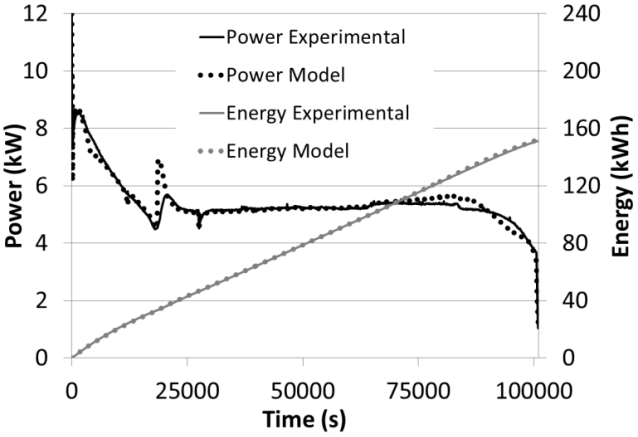

Figure 6. Power and energy comparison.

Figure 5 shows that outlet temperature of the HTF is reproduced perfectly with the model. However, since the temperature span between the inlet and outlet is small, a small deviation between

real and simulated temperatures can imply significant differences in the thermal power. Figure 6 represents the experimental and theoretical power, as well as the energy. A deviation of less than 1% in the total energy exchanged is observed.

Figure 6 shows that at the end of the latent heat transfer phase the thermal power decreases substantially. According to the model, this point is where the adjacent ice layers start to touch.

The greatest deviation between the model and experimental results happens at the moment of the nucleation. Experimentally, nucleation is not instantaneous in all the tubes of the tank. This aspect cannot be introduced in the model unless all of the tubes are modelled. Nevertheless, in terms of energy, which is the most interesting point when working on a system level, this aspect is negligible.

6. Conclusion

In this study, a dynamic model for the charging of an internal-melt-ice-on-coil tank has been developed and validated with experimental measurements.

Three finite methods have been analyzed to calculate the transport equation inside the tube. Euler's Method has finally been chosen since it does not introduce oscillations, and the small diffusion which is introduced partially compensates the neglected axial diffusion.

The model calculates the outlet temperature of the HTF for a single tube. The results show that the outlet temperature of the tank, which comes from a common collector of all of the coils, can be reproduced very well with a single tube model. Furthermore, the model has helped to understand the end of the latent heat transfer process. At the end of the charge tests, adjacent ice layers start to touch and reduce rapidly the thermal power which is transferred to the HTF.

The model calculates very well the temperature profile of the HTF, the ice growth and the thermal power. Thus, it can be useful for the design and sizing of ice-storage tanks.

The calculation of the nucleation temperature has not been implemented yet, due to its complexity and random characteristics. The nucleation temperature is thus an experimental input, but in future investigations a correlation might be introduced depending on the mass flow rate and inlet temperatures of the HTF among other parameters.

References

[1] Cabeza L F and Mehling H 2008 *Heat and Cold Storage with PCMs. An Up to Date Introduction into Basics and Applications*, Springer, Heat and Mass Transfer series. ISBN 978-3-540-68556-2

[2] ASHRAE 2007 *ASHRAE Handbook – HVAC Applications.*

[3] Zalba B, Marín J M, Cabeza L F and Mehling H 2003 Review on thermal energy storage with phase change: materials, heat transfer analysis and applications *Applied Thermal Engineering* 23, pp. 251-283

[4] Dincer I and Rosen M A 2011 *Thermal Energy Storage, Systems and Applications* John Wiley and Sons (Chichester)

[5] López-Navarro A, Biosca-Taronger J, de Rosa J, Martínez-Galván I, Esteban-Matías J C and Payá J 2011 Analysis of an experimental ice-storage installation *Eurotherm Seminar n° 93 Thermal energy storage and transportation: materials, systems and applications* (Bordeaux, France)

[6] CALMAC ICEBANK. 2011. Available at <www.calmac.com>.

[7] Tannehill J, Anderson D and Pletcher R 1997 *Computational Fluid Mechanics and Heat Transfer* (Philadelphia: Taylor and Francis)

[8] Gebhart B and Mollendorf J C 1978 Buoyancy-induced flows in water under conditions in which density extrema may arise *J. Fluid Mech.* 89 part 4, pp. 673-707

[9] Chen S L and Lee T S 1998 Astudy of supercooling phenomenon and freezing probability of water inside horizontal cylinders *Int. J. Heat Mass Transfer* 41, pp. 769-783